ISSN 1070-3284, Russian Journal of Coordination Chemistry, 2015, Vol. 41, No. 2, pp. 135–141. © Pleiades Publishing, Ltd., 2015.

Synthesis, Structure, and Luminescent Properties of a Novel Binuclear Gd(III) Compound[1]

Z. H. Xu[a], X. M. Xie[b], L. Z. Wu[a], M. Y. Liu[a], L. C. Wang[a], Y. Xu[a], L. Liu[a], and L. R. Yang[a, *]

[a] *Henan Key Laboratory of Polyoxometalates, College of Chemistry and Chemical Engineering, Henan University, Kaifeng, 475004 P.R. China*

[b] *College of Pharmacy, Henan University, Kaifeng, 475004 P.R. China*

**e-mail: lirongyang@henu.edu.cn*

Received July 13, 2014

Abstract—The compound $[Gd_2(PZDA)_3(H_2O)]_n$ (**I**), where H_2PZDA = 2,3-pyrazinedicarboxylic acid, was synthesized under hydrothermal conditions and characterized by elemental analysis, infrared spectrometry, thermogravimetric analysis and single crystal X-ray diffraction (CIF file CCDC no. 848802). In **I**, Gd(III) centers adopt eight-coordinated and nine-coordinated modes to construct distorted triangular dodecahedral and tricapped trigonal prism configurations, respectively. Three-dimensional (3D) structure of the compound is formed through C–H···π interactions and π–π stacking. Measurement of the luminescent property at room temperature shows that the as-synthesized compound presents good selectivity towards Pb^{2+} ion, suggesting that it may be promising potential as selective luminescent probes of Pb^{2+} ion.

DOI: 10.1134/S1070328415020116

INTRODUCTION

Metal-organic frameworks (MOFs) are currently one of the considerable significance owing to the combination of inorganic and organic fragments that may generate a huge number of novel architectures in the fields of inorganic and material science [1–3]. MOFs may allow the manipulation of some specific functionalities based on rational design strategies for assembling porous materials to target some specific functionalities as well as potentially industrial applications in gas storage and separation, catalysis, guest-exchange, molecular recognition, magnetic properties and selective luminescent probes [4–11]. Lanthanide metal ions present various coordination numbers and geometries, and the highly localized *f* electrons of lanthanide compounds allow *f–f* transitions, which are in association with the emission behavior of lanthanide ions within a narrow wavelength ranges results in high quantum yields. These MOFs based on lanthanide-containing compounds are intriguing and remarkably suitable for the development of optical devices and tunable luminescent sensors as well as probes for chemical species [12–15]. Selection of suitable ligands with fixed geometry and variable coordination modes is very important for the design and synthesis of luminescent MOFs with interesting geometric configurations. 2,3-Pyrazinedicarboxylic acid (H_2PZDA) and its deprotonated anions behave as multifunctional ligands to act as bridging ligands in metal compound with six potential coordination sites involving the oxygen atoms of the carboxylic groups and the nitrogen atoms of the pyrazine ring [16–19]. A wide range of applications have been reported for these compounds in industry catalysis, medicine, luminescent properties and molecular recognitions processes in biological systems as well as in specifically material sciences [20–24]. Here we report the synthesis, crystal structure, thermal analyses and photoluminescence property of the compound $[Gd_2(PZDA)_3 \cdot H_2O]_n$ (**I**).

EXPERIMENTAL

General procedures. Reagents were readily available from commercial sources and were used without further purification. Elemental analysis was performed with a PerkinElmer 240C elemental analyzer. Fourier transform infrared (FT–IR) were recorded with an AVATAR 360 FT–IR spectrometer (KBr pellets, in the region of 4000–400 cm^{-1}). The crystal structure was determined with a Bruker Smart CCD X-ray single-crystal diffractometer. Fluorescent data were collected with an F-7000 FL spectrophotometer at room temperature. Thermogravimetric (TG) and differential thermogravimetric (DTG) analyses were conducted with a PerkinElmer TGA7 system under flowing N_2 stream (flow rate 10 mL/min) from room temperature to 1000°C at a heating rate of 10°C/min.

Synthesis of compound I. A mixture of pyrazine-2,3-carboxylic acid (0.0841 g, 0.5 mmol), $Gd(NO_3)_3 \cdot 6H_2O$ (0.2167 g, 0.5 mmol), and water (10 mL) was homogenized by stirring for 30 min, then transferred into 25 mL Teflon-lined stainless steel autoclave under autogenous pressure at 160°C for 4 days. After cooling

[1] The article is published in the original.

Table 1. Crystallographic data and refinement parameters for compound **I**

Parameter	Value
Formula weight	828.79
Temperature, K	296(2)
Crystal system	Monoclinic
Space group	$P2_1/c$
a, Å	7.9868(6)
b, Å	26.4375(19)
c, Å	11.6554(8)
β, deg	107.0940(10)
Z	4
ρ_{calcd}, Mg/m^3	2.340
F(000)	1552
Crystal size, mm	0.48 × 0.45 × 0.22
θ Range for data collection, deg	1.54–25.00
Limiting indices	$-9 \le h \le 8$, $-31 \le k \le 30$, $-13 \le l \le 13$
Reflections collected/unique (R_{int})	11826/4146 (0.0228)
Data/restraints/parameters	4146/0/352
Goodness-of-fit on F^2	1.255
Volume, Å^3	2352.3(3)
Final R indices ($I > 2\sigma(I)$)	R_1 =0.0293, wR_2 = 0.0790
R indices (all data)	R_1 =0.0328, wR_2 = 0.0884
Largest diff. peak and hole, e Å^{-3}	1.118 and −1.658

$w = 1/[\sigma^2(F_o^2) + (0.0454P)^2 + 8.1245P]$ with $P = (F_o^2 + 2F_c^2)/3$.

the reaction system to room temperature at a rate of 5°C/h, yellow block crystals were isolated.

For $C_{18}H_6N_6O_{13}Gd_2$

anal. calcd., %:	C, 26.09;	H, 0.73;	N, 10.14.
Found, %:	C, 26.13;	H, 0.69;	N, 10.15.

IR spectrum (ν, cm^{-1}): 3454 b, 3305 w, 3226 w, 3070 w, 1612 s, 1560 s, 1527 s, 1495 w, 1434 m, 1417 m, 1356 m, 1304 w, 1260 w, 1150 m, 1085 m, 1045 w, 948 w, 868 m, 846 m, 815 w, 798 w, 715 m, 698 m, 652 m, 629 w, 593 m, 551 m, 491 w, 459 w.

X-ray structure determination. Suitable single crystal of the compound of dimensions 0.48 × 0.45 × 0.22 mm was mounted on a Bruker Smart CCD X-ray single-crystal diffractometer. Reflection data was at 296(2) K using graphite monochromated MoK_α radiation (λ = 0.71073 Å). All 4146 independent reflections were collected in a range of 1.54°–25.00° and determined in the subsequent refinement. Multi-scan empirical absorption corrections were applied to the data using the SADABS [25]. The crystal structure was solved by direct methods and Fourier synthesis. Positional and thermal parameters were refined by the full-matrix least-squares method on F^2 using the SHELXTL software package. All non-hydrogen atoms were refined anisotropically and all hydrogen atoms were determined with theoretical calculations and refined isotropically. A summary of the key crystallographic information is given in Table 1. Selected bond lengths and band angles for compound **I** are listed in Table 2.

Supplementary material has been deposited with the Cambridge Crystallographic Data Centre (no. 848802; deposit@ccdc.cam.ac.uk or http://www.ccdc.cam.ac.uk).

RESULTS AND DISCUSSION

The structure of compound **I** is identified by satisfactory elemental analysis as well as FT–IR and X-ray analyses. High yield of the product indicates that **I** is thermodynamically stable under the reaction conditions. The IR spectrum of **I** recorded in the range of 4000–400 cm^{-1} suggests that the $PZDA^{2-}$ ligands coordinate to the central Gd^{3+} ions. The infrared spectrum of **I** is compared with those of the original ligands. The strong broad band around 3454 cm^{-1} indicates that the existence of water molecules in coordination. For the coordination modes of carboxylate group, the difference between the asymmetric (ν_{as}) and symmetric (ν_s) carboxylate stretches ($\Delta\nu = \nu_{as} - \nu_s$) are often used. Strong absorption bands at 1695 and 1395 cm^{-1} correspond to the asymmetric and symmetric $\nu_{as}(COO^-)$ vibrations of the free $PZDA^{2-}$ ligand. After coordination to the Gd^{3+} ions, both of the bands shift to lower wave numbers and are observed at 1560 and 1356 cm^{-1}, respectively. The separation between $\nu_{as}(COO^-)$ and $\nu_s(COO^-)$ ($\Delta\nu_s$ = 204 cm^{-1}) indicates that bidentate bridging coordination mode for the $PZDA^{2-}$ ligand exists [26]. The weak band is observed at 459 cm^{-1} of the compound that corresponds to the Gd–O stretching vibration.

The coordination environment of Gd(III) centers in the compound is shown in Fig. 1a, where gadolinium entities are connected with carboxylic oxygen atoms in two types of coordination environments. Namely, Gd(1) is eight-coordinated with eight oxygen donors to construct a distorted triangular dodecahedral geometry, whereas Gd(2) is nine-coordinated with the nine donor sets to show tricapped trigonal prizm configurations probably. Around Gd(1) ion, there exist five $PZDA^{2-}$ anions: one adopts pentadentate A mode (connect with two Gd(2) and one Gd(1)), two adopt tetradentate B mode (connect with two Gd(2) and two Gd(1)), and two adopt heptadentate C mode (connect with two Gd(2) and two Gd(1)) and the rest coordination atom deriving from one molecule of terminal water, whereas six $PZDA^{2-}$ anions

Table 2. Selected bond lengths (Å) and band angles (deg) for compound **I***

Bond	*d*, Å	Bond	*d*, Å
Gd(1)–O(3)	2.288(4)	Gd(2)–O(6)	2.417(4)
Gd(1)–O(12)$^{\#1}$	2.306(4)	Gd(2)–O(1)	2.426(4)
Gd(1)–O(5)$^{\#2}$	2.350(4)	Gd(2)–O(9)	2.435(4)
Gd(1)–O(9)	2.395(4)	Gd(2)–O(8)$^{\#3}$	2.461(5)
Gd(1)–O(7)	2.405(4)	Gd(2)–O(7)$^{\#3}$	2.520(4)
Gd(1)–O(1*w*)	2.407(4)	Gd(2)–O(2)	2.686(4)
Gd(1)–O(6)	2.463(4)	Gd(2)–O(11)$^{\#3}$	2.254(4)
Gd(1)–O(2)	2.516(4)	Gd(2)–O(4)$^{\#4}$	2.284(4)
Angle	ω, deg	Angle	ω, deg
O(3)Gd(1)O(12)$^{\#1}$	98.05(16)	O(11)$^{\#3}$Gd(2)O(7)$^{\#3}$	95.48(15)
O(3)Gd(1)O(5)$^{\#2}$	82.86(16)	O(4)$^{\#4}$Gd(2)O(7)$^{\#3}$	126.88(15)
O(12)$^{\#1}$Gd(1)O(5)$^{\#2}$	149.19(16)	O(6)Gd(2)O(7)$^{\#3}$	94.25(13)
O(3)Gd(1)O(9)	91.17(14)	O(1)Gd(2)O(7)$^{\#3}$	77.88(14)
O(12)$^{\#1}$Gd(1)O(9)	136.98(15)	O(9)Gd(2)O(7)$^{\#3}$	137.88(13)
O(5)$^{\#2}$Gd(1)O(9)	73.51(15)	O(8)$^{\#3}$Gd(2)O(7)$^{\#3}$	52.00(14)
O(3)Gd(1)O(7)	152.10(14)	O(11)$^{\#3}$Gd(2)O(2)	147.64(15)
O(12)$^{\#1}$Gd(1)O(7)	94.66(15)	O(4)$^{\#4}$Gd(2)O(2)	125.24(14)
O(5)$^{\#2}$Gd(1)O(7)	73.68(15)	O(6)Gd(2)O(2)	66.89(13)
O(9)Gd(1) O(7)	96.31(14)	O(1)Gd(2)O(2)	50.71(13)
O(3)Gd(1)O(1*w*)	85.81(15)	O(9)Gd(2)O(2)	63.69(12)
O(12)$^{\#1}$Gd(1)O(1*w*)	74.22(16)	O(8)$^{\#3}$Gd(2)O(2)	111.99(13)
O(5)$^{\#2}$Gd(1)O(1*w*)	75.14(16)	O(7)$^{\#3}$Gd(2)O(2)	74.21(13)
O(9)Gd(1)O(1*w*)	148.64(15)	O(11)$^{\#3}$Gd(2)O(6)	83.83(15)
O(7)Gd(1)O(1*w*)	73.90(15)	O(4)$^{\#4}$Gd(2)O(6)	138.35(15)
O(3)Gd(1)O(6)	138.14(14)	O(11)$^{\#3}$Gd(2)O(1)	158.26(16)
O(12)$^{\#1}$Gd(1)O(6)	74.31(15)	O(4)$^{\#4}$Gd(2)O(1)	82.07(15)
O(5)$^{\#2}$Gd(1)O(6)	124.47(15)	O(6)Gd(2)O(1)	117.04(14)
O(9)Gd(1)O(6)	71.09(14)	O(11)$^{\#3}$Gd(2)O(9)	120.75(15)
O(7)Gd(1)O(6)	69.36(13)	O(11)$^{\#3}$Gd(2)O(4)$^{\#4}$	85.73(16)
O(1*w*)Gd(1)O(6)	128.60(15)	O(8)$^{\#3}$Gd(2)O(11)$^{\#3}$	82.20(16)
O(3)Gd(1)O(2)	69.16(14)	O(4)$^{\#4}$Gd(2) O(8)$^{\#3}$	75.88(16)
O(12)$^{\#1}$Gd(1)O(2)	77.39(15)	O(4)$^{\#4}$Gd(2)O(9)	80.07(14)
O(5)$^{\#2}$Gd(1)O(2)	130.10(15)	O(1)Gd(2)O(9)	74.74(14)
O(9)Gd(1)O(2)	66.92(13)	O(1)Gd(2) O(8)$^{\#3}$	77.41(15)
O(7)Gd(1)O(2)	138.23(14)	O(6)Gd(2)O(9)	71.23(14)
O(1*w*)Gd(1)O(2)	138.73(14)	O(6)Gd(2) O(8)$^{\#3}$	141.58(15)
O(6)Gd(1)O(2)	69.01(13)	O(9)Gd(2) O(8)$^{\#3}$	145.27(14)

* Symmetry transformations used to generate equivalent atoms: $^{\#1}$ $x + 1, -y + 3/2, z + 1/2$; $^{\#2}$ $x, -y + 3/2, z–1/2$; $^{\#3}$ $x, -y + 3/2, z + 1/2$; $^{\#4}$ $x - 1, y, z$.

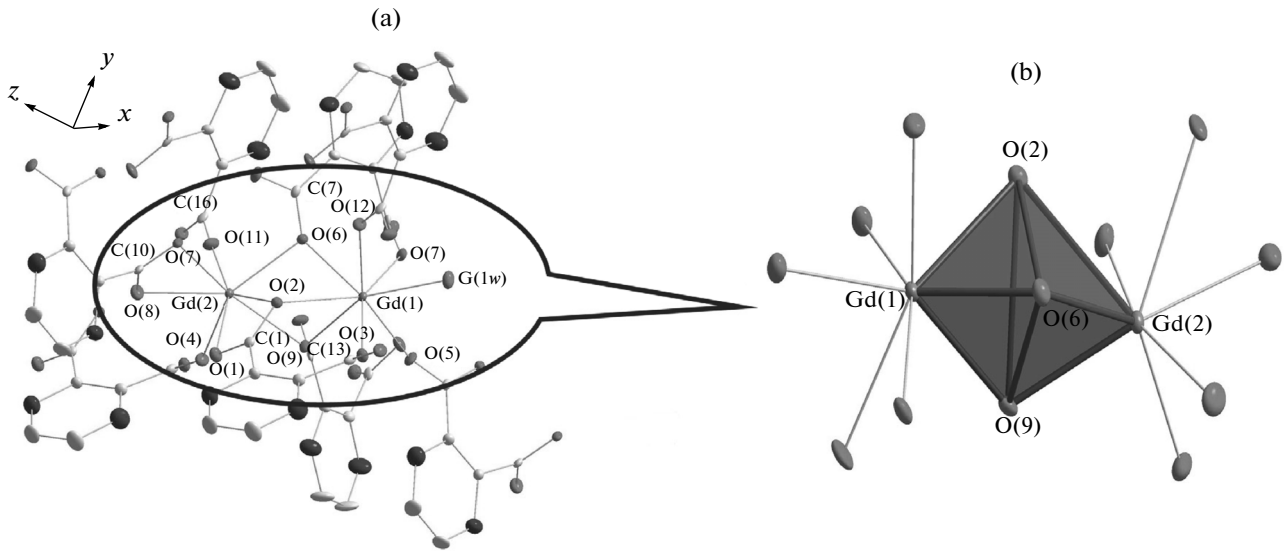

Fig. 1. Coordination environment of the compound with thermal ellipsoids at 30% probability (a) (the asymmetric unit and the related coordination atoms are labeled; lattice water and hydrogen atoms are omitted for clarity); two Gd ions and three O atoms form a trigonal bipyramid Gd_2O_3 grid (b).

surround Gd(2) ion *via* two $PZDA^{2-}$ anions in A mode, B mode, and C mode, respectively. Typical coordination modes of the $PZDA^{2-}$ anions in the compound are below:

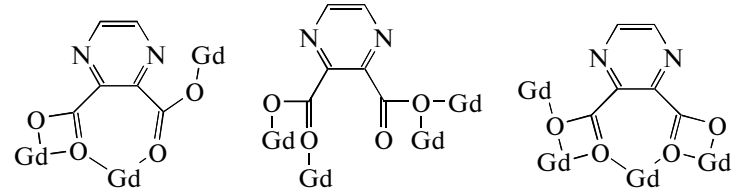

The Gd–O bond lengths in the present work range from 2.254(4) (Gd(2)–O(11)) to 2.686(4) Å (Gd(2)–O(2)), which are consistent with the previous work for the gadolinium involved compounds [27]. Gd(1) and Gd(2) are connected through three oxygen atoms (O(2), O(6), and O(9)) from three $PZDA^{2-}$ ligands in μ_2-bridging fashion (Gd(1)–O(6), Gd(1)–O(2), Gd(1))–O(9), Gd(2)–O(6), Gd(2)–O(2), and Gd(2)–O(9) are 2.463(5), 2.516(5), 2.396(4), 2.416(4), 2.686(4), and 2.435(4) Å) to form a trigonal bipyramid Gd_2O_3 grid (Fig. 1b). The two crystallographically independent Gd^{3+} ions are well-separated with the nonbonding distances of 3.771(4) Å. Based on the homometallic building block of $[Gd_2(PZDA)_3(H_2O)]_n$, the compound gives rise to an infinite one-dimensional $(Gd–(O–C–O)_2–Gd)_\infty$ wavy chain through μ_2-(η^1-O), (η^1-O') carboxylate bridges (Fig. 2a). Furthermore, the adjacent one-dimensional chains are linked by μ_2-(η^1-O), (η^1-O') oxygen bridges from $PZDA^{2-}$ anions to complete the two-dimensional (2D) highly ordered layer framework (Fig. 2b). The neighboring 2D layers are connected through π–π stacking with the distance of 3.923 Å between the parallel pyrazine rings and weak C–H···π interactions with the distance of 3.608 Å of the parallel pyrazine rings between the adjacent layers to assemble a 3D supramolecular framework (Fig. 3).

The TG and DTG curves of the compound indicate that the compound decomposes in three steps (Fig. 4). The first weight loss stage has a decomposition temperature range of 25–271°C with a weight loss of 2.14%. This corresponds to the loss of part of one molecule of water (theoretical loss is 2.17%). The second weight loss stage has a decomposition temperature range of 271–602°C with a weight loss of 40.24%. This can be assigned to the decomposition of two $PZDA^{2-}$ ligands (theoretical loss is 39.59%). The fragments of $PZDA^{2-}$ (without three oxygen atoms) ligands decompose at 603–1000°C with a weight loss of 12.20% (theoretical loss is 14.01%). The fact that the ligands lose at a higher temperature suggests that they are tightly coordinated with the Gd^{3+} ions. The decomposition product was identified as Gd_2O_3

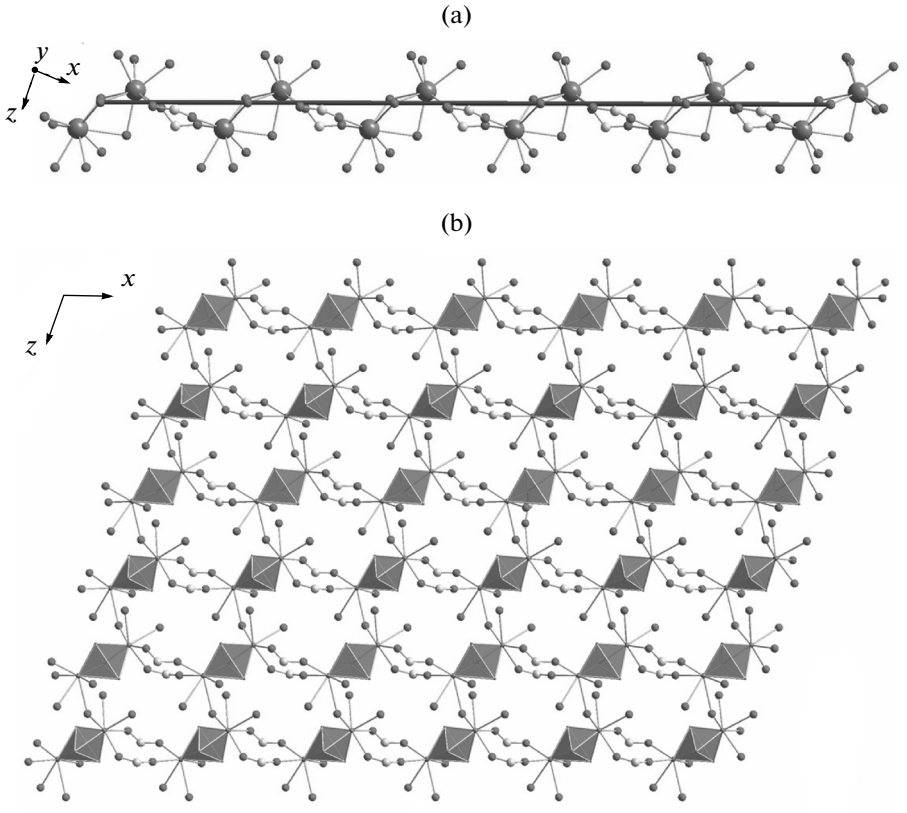

Fig. 2. Figure showing the one-dimensional $(Gd–(O–C–O)_2–Gd)_\infty$ wavy chain (a); view of the 2D layer structure of the compound (b).

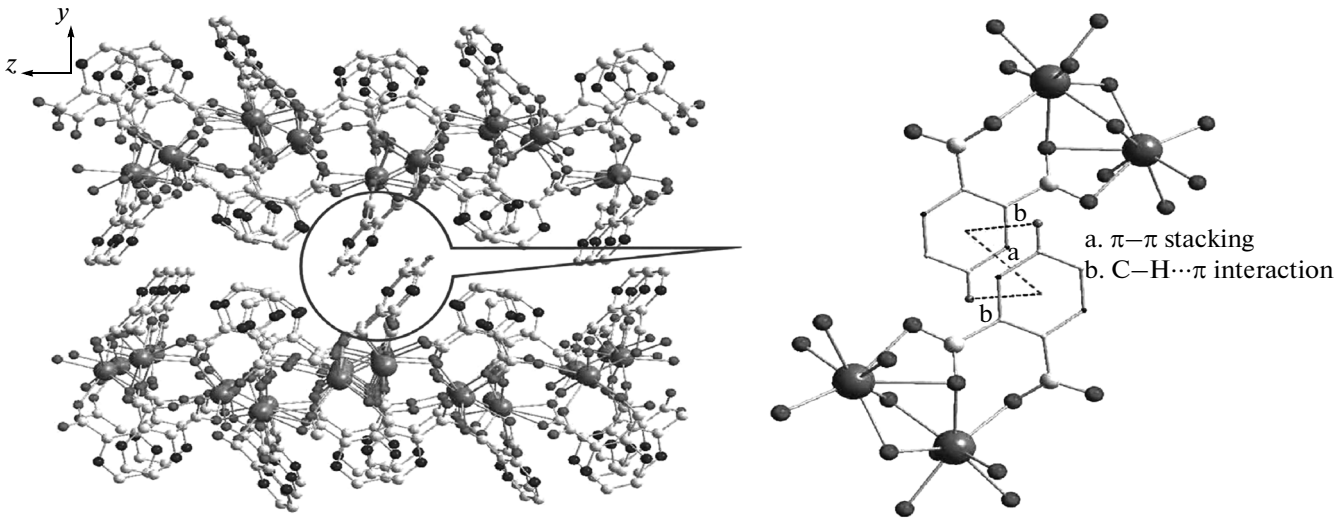

Fig. 3. C–H···π interactions and π–π stacking in the compound presenting 3D network viewed from *x* axis direction.

(45.42%), which is close to the calculated remnant weight of 45.21%.

As reported in references, the lanthanide ions are useful as luminescent probes and the lanthanide centered emission can be sensitized by molecule of ligands using the π electrons. Significant emission, characteristic of the lanthanide ions, may occurred by employing suitable ligands that can absorb and transfer the

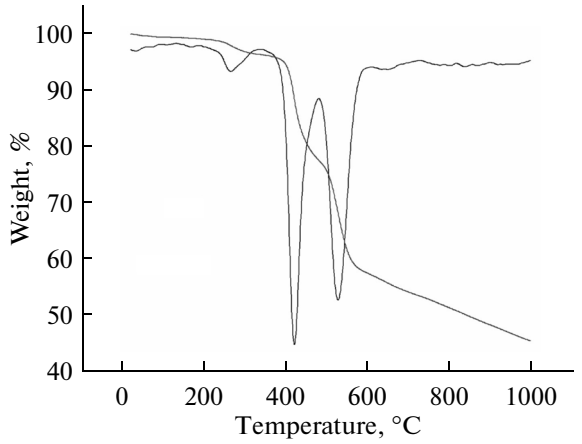

Fig. 4. TG and DTG curves of the compound.

energy to the central lanthanide ions. Generally, in coordination compound, the ligand is excited to the singlet state, where part of the energy is transferred to the triplet state through inter system crossing. When the energy levels are favorable, the triplet excited state can transfer the energy to the metal centers, resulting in metal centered luminescence [28, 29]. The transfer of energy can be identified by the suppressing of the intra-ligand emission in the luminescence spectra. For the present the compound, the $PZDA^{2-}$ anion which absorb strongly in the UV region can sensitize the lanthanide ion. To examine the possibility of modification of the luminescent properties through cations exchange, the solid sample of the compound was immersed in CH_3OH (10^{-4} M) containing various metal cations to generate solutions at room tempera-

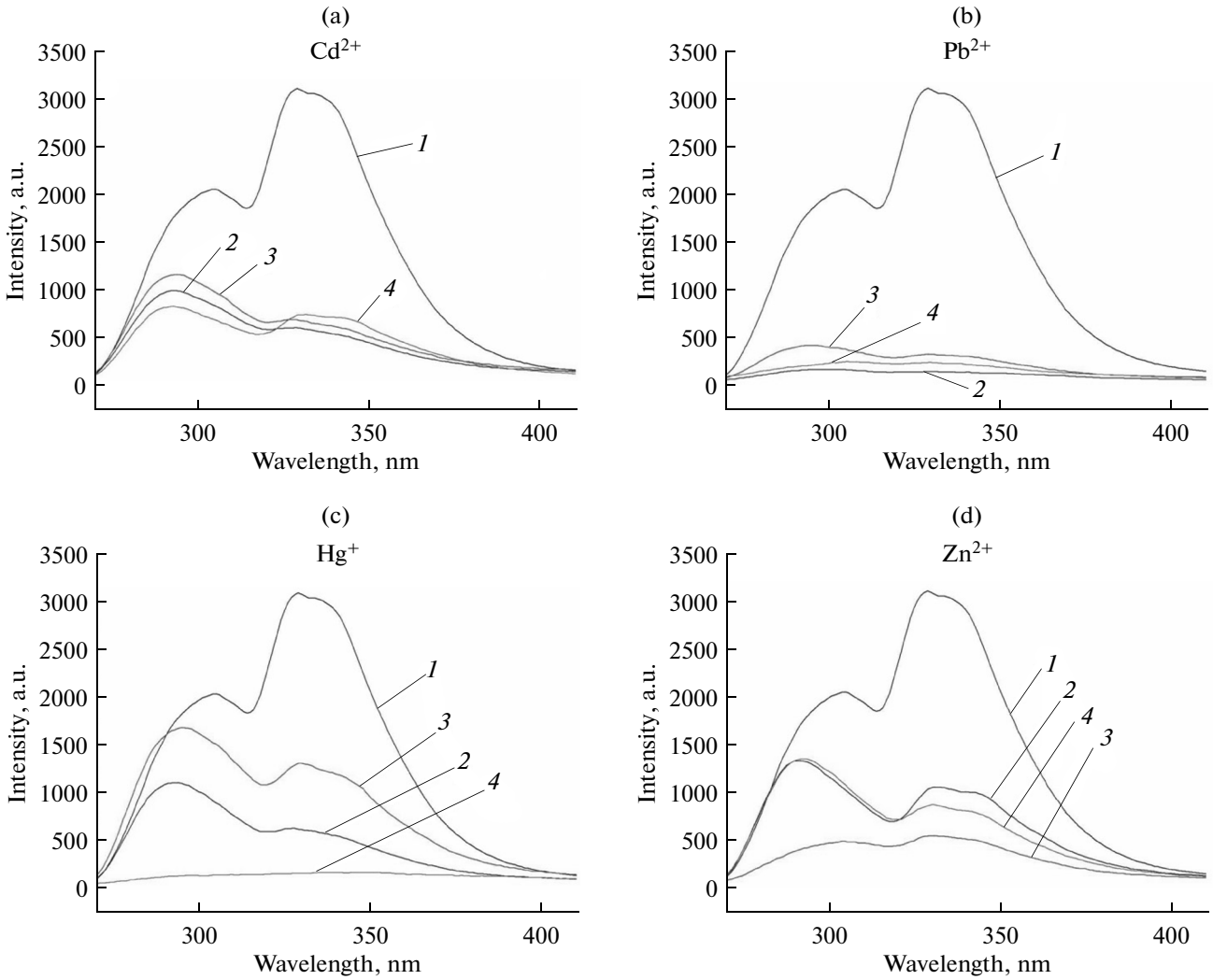

Fig. 5. Luminescent spectrum of the compound at 305 and 330 nm in CH_3OH at room temperature upon the addition of Cd^{2+} (a), Pb^{2+} (b), Hg^{+} (c), and Zn^{2+} (d) ions (excited at 226 nm) (no addition (*1*); 10^{-4} (*2*); 2×10^{-4} (*3*); 3×10^{-4} mol/L (*4*)).

ture. Emission spectrum of the compound in the presence of Cd^{2+}, Pb^{2+}, Hg^{+}, and Zn^{2+} ions with respect to the original compound are illustrated in Fig. 5. All the emission intensities of the compound decreased upon the addition of 1×10^{-3}–3×10^{-3} mol/L of Cd^{2+} ($Cd(CH_3COO)_2$), Pb^{2+} ($Pb(CH_3COO)_2$), Hg^{+} ($HgNO_3$) and Zn^{2+} ($Zn(CH_3COO)_2$) with respect to compound **I**. As the concentration of Hg^{+} ($HgNO_3$) was controlled at 3×10^{-3} mol/L, the emission spectrum at 305 and 330 nm (excited at 226 nm) of the compound quenched completely, which may be due to the $n^* \longrightarrow n$ or $\pi^* \longrightarrow \pi$ transition. Particularly, when adding 1×10^{-3}–3×10^{-3} mol/L of Pb^{2+} ($Pb(CH_3COO)_2$), the luminescent intensities of compound **I** decrease rapidly. The fluorescence quenching of compound was perhaps due to the interaction of Pb^{2+} with the original compound. According to the above results, the emission of compound **I** may be assigned to the ligand-to-metal charge-transfer bands (LMCT) [30–32].

In summary, $[Gd_2(PZDA)_3(H_2O)]_n$ is successfully synthesized under hydrothermal method. based on the analysis of X-ray crystallography, compound **I** shows one-dimensional wavy chains and two-dimensional layers as well as three-dimensional networks which are formed through C–H···π interactions and π–π stackings. The luminescent properties of compound **I** shows selectivity towards Pb^{2+} ion, which may be considered as selective luminescent probes for Pb^{2+} ion.

ACKNOWLEDGMENTS

This work was supported by the Natural Science Foundation of Henan Province, P.R. China (nos. 13A150056 and 122102210174) and the 2014 Innovative and Entrepreneurial Program of Henan University Students (14NB036).

REFERENCES

1. Yaghi, O.M., O'Keeffe, M., Ockwig, N.W., et al., *Nature*, 2003, vol. 423, no. 6941, p. 705.
2. McKinlay, A.C., Morris, R.E., Horcajada, P., et al., *Angew. Chem. Int. Ed.,* 2010, vol. 49, no. 36, p. 6260.
3. Jiang, H.L. and Xu, Q., *Chem. Commun.*, 2011, vol. 47, no. 12, p. 3351.
4. Hollingsworth, M.D., *Science*, 2002, vol. 295, no. 5564, p. 2410.
5. Huang, Y., Zhou, J., Su, B., et al., *J. Am. Chem. Soc.*, 2012, vol. 134, no. 41, p. 17053.
6. Zhao, Q., Li, R.F., Xing, S.K., et al., *Inorg. Chem.*, 2011, vol. 50, no. 20, p. 10041.
7. Lozan, V., Loose, C., Kortus, J., et al., *Coord. Chem. Rev.*, 2009, vol. 253, no. 19, p. 2244.
8. Holliday, B.J. and Mirkin, C.A., *Angew. Chem. Int. Ed.*, 2001, vol. 40, no. 11, p. 2022.
9. Zhao, F.H., Che, Y.X., and Zheng, J.M., *Inorg. Chim. Acta*, 2012, vol. 384, p. 170.
10. Yutkin, M.P., Zavakhina, M.S., Samsonenko, D.G., et al., *Inorg. Chim. Acta*, 2013, vol. 394, p. 367.
11. Huang, W.H., Hou, L., Liu, B., et al., *Inorg. Chim. Acta*, 2012, vol. 382, p. 13.
12. Li, Y.W., Ma, H., Chen, Y.Q., et al., *Cryst. Growth. Des.,* 2011, vol. 12, no. 1, p. 189.
13. Zhang, T., Ji, C., Wang, K., et al., *Inorg. Chem.*, 2010, vol. 49, no. 23, p. 11069.
14. Wang, X.L., Qin, C., Wang, E.B., et al., *Angew. Chem.*, 2004, vol. 116, no. 38, p. 5146.
15. Zhou, X.H., Li, L., Li, A., et al., *Inorg. Chim. Acta*, 2014, vol. 413, p. 38.
16. Yang, L., Song, S., Zhang, H., et al., *Synth. Met.*, 2011, vol. 161, no. 21, p. 2230.
17. Yeşilel, O.Z., Mutlu, A., and Büyükgüngör, O., *Polyhedron*, 2008, vol. 27, no. 11, p. 2471.
18. Yeşilel, O.Z., Mutlu, A., and Büyükgüngör, O., *Polyhedron*, 2009, vol. 28, no. 3, p. 437.
19. Zheng, X.J., Jin, L.P., and Lu, S,Z., *Eur. J. Inorg. Chem.*, 2002, vol. 2002, no. 12, p. 3356.
20. Carlucci, L., Ciani, G., and Proserpio, D.M., *Coord. Chem. Rev.*, 2003, vol. 246, no. 1, p. 247.
21. Li, M., Xiang, J., Yuan, L., et al., *Cryst. Growth Des.*, 2006, vol. 6, no. 9, p. 2036.
22. Uemura, K., Chang, H.C., et al., *Angew. Chem.*, 2004, vol. 116, no. 25, p. 3331.
23. Maji, T.K., Mostafa, G., Matsuda, R., et al., *J. Am. Chem. Soc.*, 2005, vol. 127, no. 49, p. 17152.
24. Ghosh, S.K. and Bharadwaj, P.K., *Inorg. Chem.*, 2003, vol. 42, no. 25, p. 8250.
25. Sheldrick, G.M., *SHELX-97, Programs for Crystal Structure Analysis,* Göttingen: Univ. of Göttingen, 1997.
26. Chandler, B.D., Cramb, D.T., and Shimizu, G.K.H., *J. Am. Chem. Soc.*, 2006, vol. 128, no. 32, p. 10403.
27. Yang, L., Liu, L., Wu, L., et al., *Dyes Pigm.*, 2014, vol. 105, p. 180.
28. Selvin, P.R., *Nat. Struct. Mol. Biol.*, 2000, vol. 7, no. 9, p. 730.
29. Cai, M., Chen, J., and Taha, M., *Inorg. Chem. Commun.*, 2010, vol. 13, no. 1, p. 199.
30. García, C., Ferraudi, G., Lappin, A.G., et al., *Inorg. Chim. Acta*, 2012, vol. 386, p. 73.
31. Mahata, P., Ramya, K.V., and Natarajan, S., *Inorg. Chem.*, 2009, vol. 48, no. 11, p. 4942.
32. Yang, L.R., Song, S., Shao, C., et al., *Synth. Met.*, 2011, vol. 161, no. 11, p. 925.